

# Strong anharmonicity and spin-phonon coupling in the quasi-two-dimensional quantum spin system $\text{Sr}_{1-x}\text{Ba}_x\text{Cu}_2(\text{BO}_3)_2$

K.-Y. Choi,<sup>1</sup> Yu. G. Pashkevich,<sup>2</sup> K. V. Lamonova,<sup>2</sup> H. Kageyama,<sup>3</sup> Y. Ueda,<sup>3</sup> and P. Lemmens<sup>1,4</sup><sup>1</sup>*Physikalisches Institut, RWTH Aachen, D-52056 Aachen, Germany*<sup>2</sup>*A.A. Galkin Donetsk Phystech NASU, 83114 Donetsk, Ukraine*<sup>3</sup>*Institute of Solid State Physics, University of Tokyo, Kashiwanoha 5-1-5, Kashiwa, Chiba 277-8581, Japan*<sup>4</sup>*Max Planck Institute for Solid State Research, D-70569 Stuttgart, Germany*

(Received 7 April 2003; published 17 September 2003)

We report Raman-scattering measurements on the quasi-two-dimensional quantum spin system  $\text{Sr}_{1-x}\text{Ba}_x\text{Cu}_2(\text{BO}_3)_2$  ( $x=0$  and  $0.1$ ) in interlayer polarizations and temperatures between 5 K and 450 K. Upon approaching the structural phase transition at  $T_s=395$  K, a strong anharmonic softening of an interlayer mode at  $62\text{ cm}^{-1}$  is observed together with overtone features and a broadening of its linewidth. Moreover, an additional 3% softening toward low temperatures points to strong spin-phonon coupling of exchange origin. Our results suggest a significance of spin-phonon interactions, interlayer lattice dynamics, and Dzyaloshinskii-Moriya interactions to understand the magnetic behavior in this compound that has earlier been discussed in the framework of the two-dimensional Shastry-Sutherland spin system.

DOI: 10.1103/PhysRevB.68.104418

PACS number(s): 75.30.Gw, 78.30.-j, 63.20.Ls, 63.20.Ry

## I. INTRODUCTION

The quasi-two-dimensional quantum antiferromagnet  $\text{SrCu}_2(\text{BO}_3)_2$  has received considerable attention due to its relevance for the two-dimensional (2D) Shastry-Sutherland model<sup>1,2</sup> which is given by the Hamiltonian  $H=J\sum_{\text{NN}}S_iS_j+J'\sum_{\text{NNN}}S_iS_j$  where NN (NNN) stands for nearest- (next-nearest) neighbor spins. The ground state of the Shastry-Sutherland model is a direct product of dimer singlet states when the ratio  $x=J'/J$  of the next-nearest interdimer coupling  $J'$  to the nearest-neighbor intradimer coupling  $J$  is smaller than a critical value near  $0.7$ .<sup>3</sup> Furthermore, the frustration between  $J$  and  $J'$  prevents a hopping of a triplet state from one dimer to another, leading to a flat triplet branch.<sup>4</sup>

Various experiments have confirmed that the orthogonally coupled spin dimers in the crystallographic  $ab$  layer form a dimer singlet ground state with a spin gap of  $\Delta=34$  K and dispersionless elementary triplets.<sup>5,6</sup> Multiparticle bound states in both the singlet and triplet sectors as well as plateaus at  $1/8$ ,  $1/4$ , and  $1/3$  of the saturation magnetization were observed due to strong interactions between the well-localized triplet excitations.<sup>5-7</sup> In addition,  $\text{SrCu}_2(\text{BO}_3)_2$  ( $x\approx 0.63-0.68$ ) is proposed to be close to a quantum critical point ( $x_c=0.691$ ) which separates a short-range dimer phase from a long-range ordered Néel phase.<sup>4,8</sup> The existence of intermediate phases such as helical order, plaquette-singlet order, or weak columnar-dimer order has been discussed for larger  $x$ .<sup>9</sup> Experiments using magnetic susceptibility under hydrostatic pressure have found evidence for a decrease of the spin gap under pressure, i.e., the dimer ground state can at least be weakened experimentally.<sup>10</sup>

Despite the success of the 2D Shastry-Sutherland model in understanding the ground state and spin gap of  $\text{SrCu}_2(\text{BO}_3)_2$ , a lot of severe deviations show up.<sup>11</sup> At finite temperatures the significance of interlayer interactions is evident from the temperature dependence of the magnetic susceptibility.<sup>12,13</sup> Interlayer coupling destabilizes the

frustration-induced singlet dimer phase while enhancing long-range antiferromagnetic correlations.<sup>14</sup> A recent crystal structure study has revealed a displacive, second-order structural phase transition at  $T_s=395$  K.<sup>15</sup> The main structural distortion was observed as a continuous corrugation of the Cu- $\text{BO}_3$  layer in a wide temperature range below  $T_s$ . This corrugation induces a change of the interlayer interaction most clearly seen as a steplike jump in the magnetic susceptibility at  $T=T_s$ .<sup>16</sup> Furthermore, the importance of spin-phonon interactions is indicated by a substantial softening of the sound velocity both as a function of temperature and magnetic field.<sup>17</sup> This implies a sensitivity of the dimer system to specific ionic displacements. The observation of a magnetic superstructure by high-field nuclear-magnetic-resonance measurements at the  $1/8$ -magnetization plateau<sup>18</sup> further supports this evidence. Finally, neutron-scattering experiments and electron spin resonance (ESR) show multiparticle triplet bound states with an anomalous  $k$  dependence of the structure factor<sup>19,20</sup> and zero-field splitting<sup>21</sup> that is not in accordance with a pure 2D Shastry-Sutherland model.<sup>22</sup> The splitting of the triplets may be understood by taking into account a Dzyaloshinskii-Moriya (DM) interaction which partially lifts the magnetic frustration and suppresses the spin gap.<sup>20</sup>

The above-mentioned results suggest that in order to develop a closer understanding of  $\text{SrCu}_2(\text{BO}_3)_2$  the minimal model should be extended to a quasi-2D  $J$ - $J'$  model including spin-phonon coupling, lattice distortions, and DM interaction. To our present knowledge these additional terms should lead to the observed close interplay of structure and magnetism in this system. For further understanding especially Raman spectroscopy can provide valuable information, as the involved degrees of freedom can be investigated simultaneously and with an unprecedented sensitivity and resolution. In previous Raman experiments a softening of a low-frequency optic mode at  $62\text{ cm}^{-1}$  has been observed in a wide temperature interval.<sup>15</sup> Unfortunately, these experi-

ments were restricted to *ab*-plane polarizations of the incident and scattered electric-field vectors, neglecting important aspects of interlayer lattice dynamics. In this paper, we report to the best of our knowledge the first Raman-scattering data of  $\text{Sr}_{1-x}\text{Ba}_x\text{Cu}_2(\text{BO}_3)_2$  ( $x=0$  and  $0.1$ ) in interlayer polarizations. The previously observed mode shows up as an interlayer mode with a spectral weight that is two orders of magnitude larger than that of the in-plane modes. The symmetry group analysis and doping dependence identify this soft mode as an in-phase motion of almost all ions in the primitive cell along the *z* direction. Pronounced overtone features and an additional softening by 3% below a temperature scale given by the spin gap point to strong anharmonicities and spin-phonon coupling in  $\text{SrCu}_2(\text{BO}_3)_2$ . Furthermore, we substantiate the presence of the DM interaction using an analysis of the exact crystal symmetry.

## II. EXPERIMENTAL DETAILS

High quality single crystals of  $\text{Sr}_{1-x}\text{Ba}_x\text{Cu}_2(\text{BO}_3)_2$  ( $x=0$  and  $0.1$ ) were grown using a vertical traveling solvent floating-zone method from a  $\text{LiBO}_3$  flux.<sup>23</sup> Samples with typical dimension  $5 \times 5 \times 3 \text{ mm}^3$  were used for Raman-scattering measurements. The measurements were done in a continuous helium flow optical cryostat by varying temperature from 5 K to a room temperature. The high-temperature measurements from 300 K to 450 K were carried out using a heating vacuum stage. This vacuum stage is filled with argon gas in order to avoid a possible oxygen loss as well as a contamination of the Raman signal by rotational modes of  $\text{N}_2$  and  $\text{O}_2$ . Note that the studied temperature interval reaching up to 177 °C can be achieved without pumping out the sample space. Furthermore, the studied compound with a melting temperature of  $\sim 900$  °C is stable in this temperature range. The experiments were completely reversible. All spectra were taken in a quasibackscattering geometry with the excitation line  $\lambda = 514.5 \text{ nm}$  of an  $\text{Ar}^+$  laser and analyzed by a DILOR-XY spectrometer and a nitrogen cooled charge-coupled device detector. The laser power of 5 mW was focused to a 0.1-mm-diameter spot on the interlayer surface. The averaged laser power density amounts to  $\sim 70 \text{ W/cm}^2$ . Since the studied sample is semitransparent, the local overheating due to the incident light is expected to be less than 0.5 K. Thus, heating effects are not taken into account in the analysis of our results.

## III. RESULTS AND DISCUSSIONS

### A. Symmetry analysis of phonon modes

Before discussing Raman spectra we will present a group-theoretical analysis as a first step to understand the nature of the soft mode and its possible effect on the magnetic properties of  $\text{SrCu}_2(\text{BO}_3)_2$ . Our analysis is based on the result of a recent x-ray study<sup>15</sup> which provides detailed information about the temperature dependence of atomic parameters and crystal symmetry.

In the high-temperature (HT) phase  $\text{SrCu}_2(\text{BO}_3)_2$  has space group  $I4/mcm$  where Sr atoms have  $D_{4-}(2a-)$  site symmetry, Cu, B, and O1 atoms have  $C_{2v}'-(4h-)$  site sym-

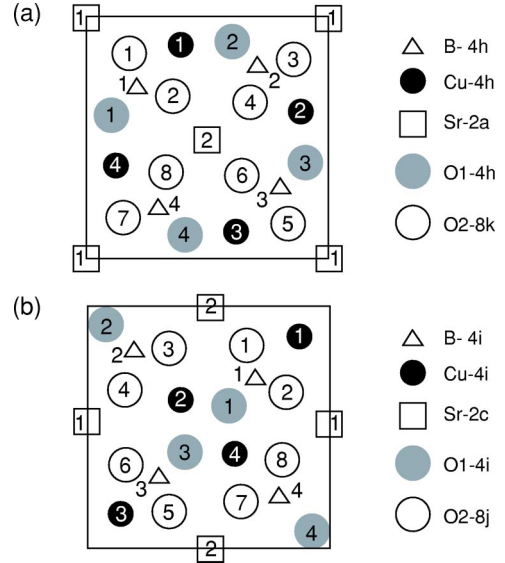


FIG. 1. (Color online) (a) Primitive unit cell and site symmetry of the atoms in the high-temperature phase (space group  $I4/mcm$ ). (b) Primitive unit cell and site symmetry of the atoms in the low-temperature phase (space group  $I\bar{4}2m$ ) of  $\text{SrCu}_2(\text{BO}_3)_2$ .

metry, and O2 atoms possess  $C_s^h-(8k-)$  site symmetry [see Fig. 1(a)]. A factor group analysis gives the experimentally observed infrared and Raman-active modes as follows:

$$\Gamma_{HT} = 5A_{1g} + A_{1u} + 6A_{2g} + 5A_{2u} + 5B_{1g} + 4B_{1u} + 5B_{2g} + B_{2u} + 6E_g + 11E_u. \quad (1)$$

According to this representation one expects 27 Raman-active modes. The space group of the low-temperature (LT) phase is a maximal nonisomorphic subgroup of the space group of high-temperature phase. This group-subgroup relation is one of the prerequisites for the application of the Landau theory for second-order phase transitions. The LT phase has space group  $I\bar{4}2m$  where Sr atoms occupy  $D_{2-}(2c-)$  site symmetry, Cu, B, and O1 atoms have  $C_s-(4i-)$  site symmetry, and O2 atoms belong to  $C_{1-}(8j-)$  site symmetry [see Fig. 1(b)]. The factor group analysis predicts

$$\Gamma_{LT} = 9A_1 + 7A_2 + 6B_1 + 10B_2 + 17E. \quad (2)$$

Subtracting the acoustic modes ( $B_2 + E$ ) one obtains 56 Raman-active modes. With decreasing temperature through the structural phase transition at  $T_s = 395 \text{ K}$  the expected evolution of phonon modes follows a subgroup connection of the space groups between HT and LT phases. In particular, in a second-order phase transition the new structure is a subgroup of the old structure. Thus, there will always be a zone-center  $A_1$  component of the soft mode below  $T_s$  regardless of the symmetry of the soft mode in the higher-symmetry phase. Furthermore, the HT phase loses  $m_z$  and  $m_x$  mirror planes, which are generators of the  $I4/mcm$  space group. The translation symmetry remains the same. The 9  $A_1$  modes of the LT phase are correlated with  $(5A_{1g} + 4B_{1u})$  modes of the HT phase. Thus, one of the four  $B_{1u}$  buckling modes at the  $\Gamma$  point of the Brillouin zone is a soft mode in the HT

phase approaching  $T_s$ . Normal coordinates of these modes are given by  $Q_h^{B_{1u}} = \frac{1}{2}(U_{1z} - U_{2z} + U_{3z} - U_{4z})$  and  $Q_k^{B_{1u}} = (1/2\sqrt{2})(U_{1z} + U_{2z} - U_{3z} - U_{4z} + U_{5z} + U_{6z} - U_{7z} - U_{8z})$  for the  $h$  and  $k$  sites, respectively. It should be noted that these modes are silent and include only the displacements of the  $h$ - and  $k$ -site ions along the  $z$  direction. Such distortions violate the  $m_z$ ,  $m_x$ , and  $m_y$  symmetry planes and preserve the  $D_{2d}$  symmetry. According to the x-ray analysis in the LT phase, some in-phase superposition of  $Q_{Cu}^{B_{1u}}$ ,  $Q_B^{B_{1u}}$ ,  $Q_{O1}^{B_{1u}}$ , and  $Q_{O2}^{B_{1u}}$  normal coordinates becomes frozen-in for temperatures below  $T_s$  [see Fig. 9(b) in Ref. 15]. Precisely, this superposition represents an order parameter of the structural phase transition. Note that Sr ions with  $a$ -site symmetry do not participate in this order parameter.

In the LT phase four  $B_{1u}$  silent modes of the HT phase become Raman-active  $A_1$  modes. The  $Q_i^{IIA_1}$  and  $Q_j^{IIIA_1}$  normal coordinates of the  $A_1$  mode correspond to  $Q_h^{B_{1u}}$  and  $Q_k^{B_{1u}}$ , respectively (see the Appendix). As it was previously mentioned this soft mode involves an in-phase motion of almost all ions in the primitive cell (except Sr ions) along the  $z$  direction. The soft mode consists of a motion of atoms with heavy mass leading to a large effective mass. Thus, the energy of the soft mode is expected to be small even at low temperatures. In addition, the  $A_1$  normal coordinates of  $Q_i^{IA_1}$ ,  $Q_j^{IA_1}$ , and  $Q_j^{IIA_1}$  contain  $xy$  components of a motion of the ions in the LT phase. Thus, we can expect a mixing of the  $xy$  and  $z$  components of the normal coordinates. However, the x-ray analysis<sup>15</sup> did not show substantial shifts of Cu, B, and O ions along  $x$  and  $y$  directions in the LT phase, if compared to the HT phase. This implies that the  $A_1$  modes hold the properties of the  $B_{1u}$  modes of the HT phase which consist of motions predominantly along the  $z$  direction. Therefore, we expect a strong anisotropic Raman scattering of the  $A_1$  modes; that is, the dominant scattering intensity should be seen in  $zz$  polarization.

At last, we mention that the 7  $A_2$  modes of the LT phase are correlated with the (6  $A_{2g} + B_{2u}$ ) modes of the HT phase, the 6  $B_1$  modes with the (5  $B_{1g} + A_{1u}$ ) modes, the 10  $B_2$  modes with the (5  $B_{2g} + 5 A_{2u}$ ) modes, and the 17  $E$  modes with the (6  $E_g + 11 E_u$ ) modes, respectively. Therefore, one expects transition-induced scattering intensity of the (4  $A_1 + B_1 + 4 B_2 + 10 E$ ) modes in the LT phase among which (4  $B_2 + 10 E$ ) are infrared active in the HT phase. The actual observability of these modes in interlayer polarizations depends on the evolution of the Raman tensor for each mode through the structural phase transition.

### B. Interlayer soft mode

Figure 2 displays Raman spectra of  $\text{SrCu}_2(\text{BO}_3)_2$  in  $(cc)$  and  $(ca)$  polarizations at 293 K and 410 K which lie below and above  $T_s = 395$  K, respectively. The corresponding data of  $\text{Sr}_{0.9}\text{Ba}_{0.1}\text{Cu}_2(\text{BO}_3)_2$  (not shown here) show only tiny frequency shifts of some phonon modes with respect to the undoped sample. Note here that the  $c$  axis is perpendicular to the layer. Thus, these data provide mainly information about interlayer lattice dynamics. For Raman spectra in intralayer

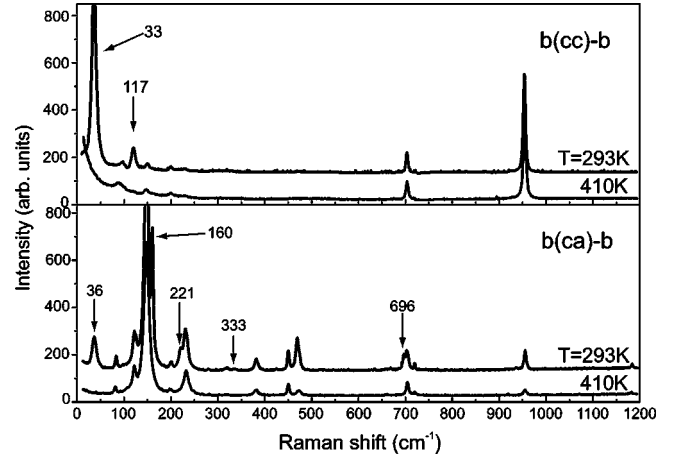


FIG. 2. Raman spectra of  $\text{SrCu}_2(\text{BO}_3)_2$  for two interlayer polarizations at 293 K and 410 K, respectively. The arrows indicate additional modes which appear for temperatures  $T < T_s = 395$  K. Note that the intensity of these modes in  $b(ca)-b$  polarization is typically very weak.

scattering geometries we refer to Refs. 7, 11, and 15. At room temperature two additional modes at 33 and  $117 \text{ cm}^{-1}$  appear in the  $(cc)$  polarization while five additional modes (see the arrows in Fig. 2) can be seen in the  $(ca)$  polarization. Noticeably enough, four modes at 160, 221, 333, and  $696 \text{ cm}^{-1}$  in the  $(ca)$  polarization turn up as a shoulder of high-temperature phonon modes. The appearance of additional modes in the  $(ca)$  polarization can be ascribed to a mixing of weak  $ab$ -plane motions with a strong modulation of the susceptibility tensor by a displacement along the  $c$  direction. A strong displacement along the  $c$  direction will cause infrared-active modes of the HT phase consisting of an  $ab$ -plane motion to become Raman active in the LT phase. As listed in the Appendix, the normal coordinates of the doubly degenerated  $E_u$  mode include an  $xy$ -plane motion of the  $h$ -site ions while that of the  $E_g$  mode contains a motion of the  $h$ -site ions along the  $z$  direction. Therefore, the observed modes in the  $(ca)$  polarization can be ascribed to an enhancement of Raman tensors of the  $E_u$  modes in the LT phase. Interestingly enough, the observed  $E_u$  mode in the LT phase is energetically very close to the frequency of the  $E_g$  mode in the HT phase. The shoulder structure of the additional modes with weak intensity indicates that the symmetry breaking is rather weak and that the crystal symmetries of the HT and LT phases are closely related. In contrast, the 33- and  $117\text{-cm}^{-1}$  modes in the  $(cc)$  configuration and the  $36\text{-cm}^{-1}$  mode in the  $(ca)$  polarization are no longer observable in the HT phase. Thus, these modes are attributed to a soft mode that results from the structural phase transition. This is due to the fact that in a second-order structural phase transition an optic soft mode is always Raman active in the lower-symmetry phase but it is not always Raman active in the higher-symmetry phase. The 33- and  $36\text{-cm}^{-1}$  modes in two different polarizations have close peak energies, indicating the same origin. The intensity of the  $36\text{-cm}^{-1}$  mode in the  $(ca)$  polarization amounts to 10% of that of the  $33\text{-cm}^{-1}$  mode in the  $(cc)$  polarization. The corresponding mode observed in  $(aa)$  polarization has negligible intensity com-

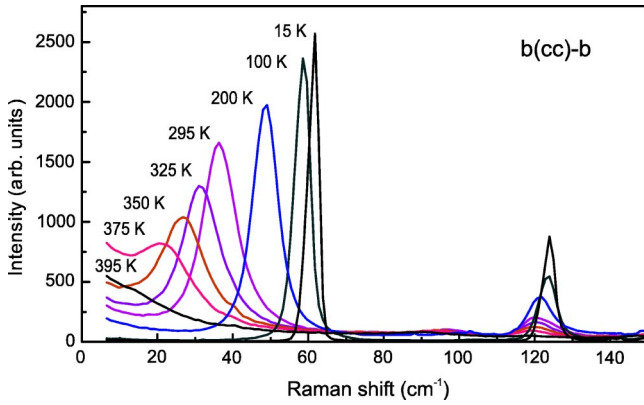


FIG. 3. (Color online) Softening of a phonon mode in (*cc*) polarization as a function of temperature. Note that an overtone of the  $62\text{-cm}^{-1}$  mode is present at  $124\text{ cm}^{-1}$ .

pared to the mode with interlayer polarization.<sup>15</sup> This indicates an extreme anisotropy of the Raman tensor of the soft mode and is consistent with the symmetry analysis showing that the soft mode involves an in-phase motion of almost all ions in a primitive cell preferably along the *c* axis (interlayer direction). An x-ray scattering structure analysis of  $\text{SrCu}_2(\text{BO}_3)_2$  shows for  $T > T_c$  an inversion center and completely flat  $\text{CuBO}_3$  planes. For temperatures below  $T < T_c$  atomic displacements are directed perpendicular to the *ab* plane leading to a buckling of the planes.<sup>15</sup> The in-phase motion also explains why the observed energy of the soft mode in our Raman experiments is so small. In addition, we observe a slight increase in integrated intensity of almost all phonon modes upon cooling. This can be ascribed to a change of both dipole matrix elements and band energies with the structural transition. The origin of the  $117\text{-cm}^{-1}$  mode will be discussed further below.

The evolution of the low-frequency modes in (*cc*) polarization is displayed in Fig. 3. Upon approaching the phase transition the  $60\text{-cm}^{-1}$  mode at  $T = 5\text{ K}$  increases slightly up to  $62\text{ cm}^{-1}$  at  $T = 15\text{ K}$  and finally disappears into the tail of quasielastic scattering around  $T_s$  while softening roughly by  $44\text{ cm}^{-1}$ . At the same time, its linewidth broadens strongly. Interestingly enough, an overtone of the  $62\text{-cm}^{-1}$  mode is observed at  $124\text{ cm}^{-1}$ . This implies a strong anharmonicity of the soft mode. The second-order mode undergoes a small softening by  $5\text{ cm}^{-1}$ , suggesting that the original soft mode has a nearly flat dispersion with a large density of states. This can be explained as follows. The frequency of the soft mode around the Brillouin center will rapidly fall to zero as the transition is approached. In contrast, phonons at the vicinity of the zone boundary will remain robust. For first-order scattering Raman spectroscopy is sensitive to the softening of phonons near the zone center. However, the whole Brillouin zone contributes to higher-order Raman scattering. The spectral weight is proportional to the density of states if there are no interactions. Therefore, the resulting scattering intensity will be dominated by zone-boundary phonons with large spectral weights. Here we draw attention to similar phonon anomalies reported in the alternating chain system  $(\text{VO})_2\text{P}_2\text{O}_7$ . A strong anharmonic phonon at  $123\text{ cm}^{-1}$  soft-

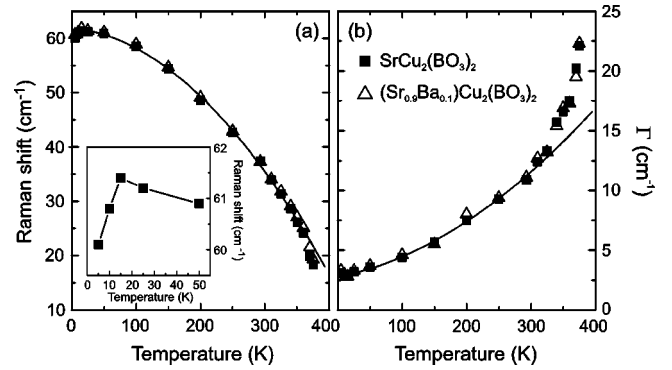


FIG. 4. (a) Temperature dependence of the soft mode. The inset shows a softening of the soft mode for temperatures  $T < 15\text{ K}$ . (b) Temperature dependence of the damping constant which is defined as the full width at half maximum. The solid lines give a fit using Eq. (3). The full square (open triangle) denotes the undoped (10% Ba doped) sample.

ens in this compound by 10%.<sup>24</sup> Most probably, this mode modulates the exchange along the alternating chain and its energy coincides with the zone-boundary energy of the singlet-triplet excitation gap  $E_{ZB} = 125\text{ cm}^{-1}$  of the spin system.<sup>25</sup> Strong spin-phonon coupling as well as the existence of a high-symmetry phase under high pressure has been attributed to the origin for the anharmonicity of optical phonons.<sup>26,27</sup> In this regard, the overtone feature of the soft mode in  $\text{SrCu}_2(\text{BO}_3)_2$  should be ascribed to the existence of a high-symmetry phase at elevated temperatures. This relies on an enhancement of anharmonic phonon-phonon interactions due to the strain induced by the buckling distortions of the LT phase. Furthermore, in the LT phase, exchange paths are strongly susceptible to ionic displacements since they will not be mutually compensated due to the lower crystal symmetry. As will be discussed in Sec. III C, special spin topology together with buckling distortions induces strong spin-phonon coupling. This suggests that the simultaneous occurrence of anharmonic phonon interactions and strong spin-phonon coupling in a low-symmetry phase may be a generic feature of low-dimensional spin gap systems.

The temperature dependence of the frequency shift and the damping constant of the soft mode is plotted in Fig. 4. Within the experimental resolution we did not detect a difference between the undoped and the 10% Ba-doped samples. This observation strongly confirms that the soft mode does not include motions of the Sr ions, consistent with the symmetry analysis. Both the peak position and the linewidth change strongly over a large temperature range between 5 K and 370 K. Such a temperature dependence can be ascribed to anharmonic terms in the vibrational potential energy. Taking into account cubic and quartic anharmonic contributions, the temperature dependence of the peak position is given by<sup>28</sup>

$$\omega(T) = \omega(0) + A \left( 1 + \frac{2}{e^x - 1} \right) + B \left( 1 + \frac{3}{e^y - 1} + \frac{3}{(e^y - 1)^2} \right), \quad (3)$$

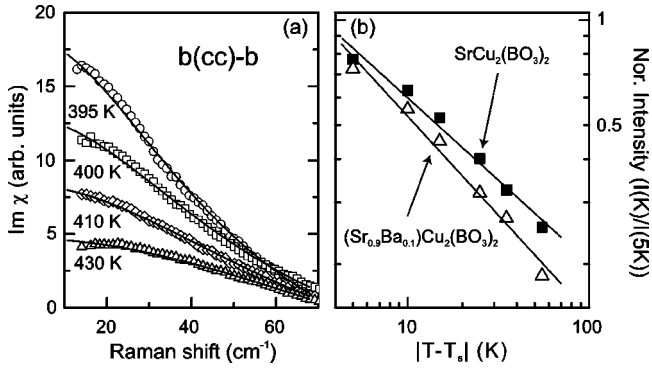


FIG. 5. (a) Low-energy Raman spectra for  $T > T_s$  after correcting with the Bose-Einstein thermal factor. The solid line is a fit with a Lorentzian line. (b) The log-log plot of the normalized intensity as a function of  $|T - T_s|$ .

where  $x = \hbar \omega(0)/2k_B T$  and  $y = \hbar \omega(0)/3k_B T$  with  $\omega(0)$ ,  $A$ , and  $B$  constants. The first term represents the frequency of soft modes at zero temperature. The second and third terms originate from the decay of an optic phonon into three- and four-phonons due to anharmonicity, respectively. In the high-temperature limit, the second and third terms vary as  $T$  and  $T^2$ , respectively. The fit of the experimental data to Eq. (3) gives  $\omega(0) = 62 \text{ cm}^{-1}$ ,  $A = -0.48 \text{ cm}^{-1}$ , and  $B = -0.07 \text{ cm}^{-1}$ . The smallness of the ratio  $B/A = 0.15$ , related to a small contribution of the four-phonon process to the softening, guarantees the validity of the fitting. Despite a reasonable agreement between the fitted curve and the experimental data in the overall temperature range one can see a deviation for temperatures above 350 K as well as at very low temperature. The temperature dependence of the linewidth can also be described using a similar relation as Eq. (3). The fitting values of the linewidth at zero temperature  $\Gamma(0)$  and the coefficients  $A$  and  $B$  are found to be 2.7, 0.24, and  $0.02 \text{ cm}^{-1}$ , respectively. This leads to a ratio  $B/A = 0.08$ , also suggesting a small contribution of the four-phonon process. The origin of the discrepancy in the ratios with respect to the behavior of frequency and linewidth is not clear. It is certainly related to the strong anharmonicity and/or spin-phonon interaction beyond this modeling. As shown in Fig. 4(b), significant deviations from the semiphenomenological model can be seen for temperatures above 310 K. The pronounced discrepancy in the high-temperature limit arises from a stronger broadening of the linewidth than a  $T^2$  dependence. This points to the necessity of higher-order terms than the four-phonon processes in the model. The observation of pronounced anharmonicity (two-phonon scattering) already demands a more elaborate modeling.

Figure 5 displays low-energy Raman spectra for temperatures above  $T_s$ . Within the accessible low-frequency resolution we have not observed a sharp central peak around  $T_s$ . Instead, a relatively broad elastic-scattering maximum is observed which is fitted well by a Lorentzian profile. The intensity is reasonably described by  $|T - T_s|^p$  with the power  $p = 0.47$  and  $0.56$  for the undoped and the 10% Ba-doped samples, respectively [see Fig. 5(b) plotted on a logarithmic scale of  $|T - T_s|$ ]. As a possible origin of the central peak the decay of a soft mode into acoustic modes or phonon density

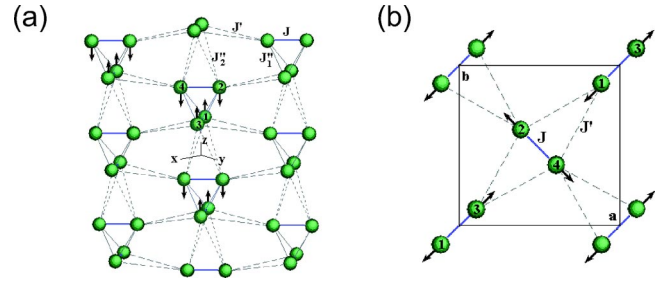


FIG. 6. (Color online) (a) Displacements of copper ions with  $Q^{II A1}$  symmetry on the background of the already existing buckling distortions. (b) Displacements of copper ions with  $Q^{I A1}$  symmetry.

fluctuations should be discussed. We notice that the observed behavior is in reasonable agreement to  $|T - T_s|^{1/2}$  which is expected within the Landau theory for structural phase transitions which are not proper ferroelastic ones.<sup>29</sup> In this case a quadratic coupling of the order parameter  $\eta$  to a permeability tensor leads to only an  $\eta^4$  contribution to the order-parameter fluctuations in the intensity of the central peak. Thus, this suggests that the observed central peak is related to a fluctuation of the order parameter.

### C. Spin-phonon coupling and effect of buckling distortions in $\text{SrCu}_2(\text{BO}_3)_2$

In dimerized spin system spin-phonon interactions play an important role in determining the magnitude of spin gap and the strength of dimerization.<sup>11</sup> Optic- and/or acoustic-phonon anomalies can accompany the onset of a dimerized state as reported in  $\text{CuGeO}_3$  (Ref. 30) and  $\text{SrCu}_2(\text{BO}_3)_2$ .<sup>31</sup> In  $\text{SrCu}_2(\text{BO}_3)_2$  the in-plane elastic constant  $c_{66}$  shows a pronounced softening of 4.5% for temperatures below 25 K (Refs. 17 and 31), which is attributed to an exchange striction coupling. Furthermore, under a magnetic field applied along the  $[100]$  direction an enormous softening of the in-plane  $c_{11}$  and  $c_{66}$  elastic constants takes place in the vicinity of the magnetization plateaus where excited triplets become highly mobile.<sup>17</sup> This highlights a close relation between spin-phonon coupling and DM interaction which promotes hopping of triplets.<sup>20,32</sup> One can also expect optic-phonon anomalies around the magnetization plateaus.<sup>32</sup> This is because the alteration of intradimer bond lengths for each site results in the alternating magnetization.

The main aspect of the structural phase transition in  $\text{SrCu}_2(\text{BO}_3)_2$  is buckling distortions due to strong anharmonicity. These lead to alternating distances between copper ions along the  $z$  direction. As Fig. 6(a) displays, in the LT phase there are two different interlayer coupling constants  $J_2''$  of longer bonding length and  $J_1'$  of shorter bonding length. At 100 K the relative distance between nearest-neighboring Cu ions along the upward and downward directions of the  $c$  axis amounts to  $\delta_z = 1.02 \text{ \AA}$ , that is, 15% of the lattice constant<sup>15</sup>  $c$  [as sketched in Fig. 6(a)]. Thus, we can safely neglect  $J_2''$ . This buckling distortion, changing the bonding angle and distance via spin-lattice interaction, can modify anisotropic magnetic properties as a function of temperature.

With the special structural topology in mind we will turn to the anomalous decrease of the optic-phonon frequency

observed in the low-temperature limit ( $T < \Delta = 34$  K). As displayed in the inset of Fig. 4(a), the peak energy of the soft mode reaches a maximum around 15 K and then softens by 3% with further lowering temperature. The energy of the soft mode  $62 \text{ cm}^{-1} = 89$  K is comparable to the nearest-neighbor intradimer coupling constant  $J = 85$  K.<sup>16</sup> Furthermore, the softening is observed for temperatures below the spin gap of 34 K. Thus, the observed softening should be attributed to a renormalization of phonon energy due to strong spin-phonon coupling. Further evidence for strong spin-phonon coupling can be provided by strong quasielastic light scattering induced by fluctuations of the energy density of the spin system.<sup>7</sup> As already shown in the symmetry analysis, the soft mode corresponds to motions of almost all ions along the interlayer direction. Consequently, the soft mode mediates all possible types of exchange interactions including the interlayer and the intralayer interactions. Since the soft mode has  $A_1$  symmetry, it suffices to consider spin-phonon coupling in the  $Q^{IIA_1}$ - and  $Q^{IA_1}$ -symmetry displacements of Cu ions. Following Miyahara *et al.*<sup>32</sup> one can derive spin-phonon coupling of the soft mode in an exchange approximation.

First, we focus on the case of the  $Q^{IIA_1}$  normal mode which includes motions of Cu, B, and O1 ions along the  $z$  axis [see Fig. 6(a)]. Spin-phonon interaction of the  $Q^{IIA_1}$  symmetry reads as follows:

$$-Q^{IIA_1} \left( \beta \frac{\delta_z}{l_{\parallel}^2} J' \sum_{\text{NNN}} \mathbf{S}_i \cdot \mathbf{S}_j + \gamma \frac{l_{\perp}^z}{l_{\perp}^2} J'' \sum_{\text{NNNz}} \mathbf{S}_i \cdot \mathbf{S}_j \right), \quad (4)$$

where NNN (NNNz) stands for next-nearest neighboring Cu ions in the  $ab$  plane (along the  $z$  direction).  $\mathbf{l}_{\perp}$  ( $\mathbf{l}_{\parallel}$ ) is the vector connecting them in the  $ab$  plane (along the  $z$  direction).  $\beta$  and  $\gamma$  denote the exponents of the distance dependence of  $J'(\mathbf{r})$  and  $J''(\mathbf{r})$ , respectively. It is worth mentioning that the soft mode of the  $Q^{IIA_1}$  symmetry does not mediate the intradimer interactions. Moreover, in the HT phase the  $Q^{IIA_1}$  type of spin-lattice interaction completely disappears because of the absence of buckling distortions ( $\delta_z = 0$ ) as well as the cancellation of the interlayer contribution by each other ( $J''_1 = J''_2$ ). Assuming that  $\beta \approx \gamma$  one sees that the contribution of the interlayer and the intralayer interactions to spin-phonon coupling in the LT phase is comparable to each other with  $l_{\perp} = 3.48 \text{ \AA}$ ,  $l_{\perp}^z = 2.81 \text{ \AA}$  and  $l_{\parallel} = 5.14 \text{ \AA}$ ,  $J' = 0.635J$ , and  $J'' = 0.09J$ .<sup>15,2</sup>

Another contribution to spin-phonon coupling comes from the  $Q^{IA_1}$ -symmetry uniform displacements of Cu-ions which consist of motions of Cu, B, and O1 ions in the  $xy$  axis [see Fig. 6(b)]:

$$-Q^{IA_1} \left( \frac{\alpha}{l} J \sum_{\text{NN}} \mathbf{S}_i \cdot \mathbf{S}_j - \beta \frac{\sqrt{l_{\parallel}^2 - l^2} - l}{l_{\parallel}^2} J' \sum_{\text{NNN}} \mathbf{S}_i \cdot \mathbf{S}_j \right), \quad (5)$$

where NN stands for nearest-neighbor Cu ions.  $\mathbf{l}$  is the vector connecting the intradimer Cu ions.  $\alpha$  denotes the exponent of the distance dependence of  $J(\mathbf{r})$ . Here note that this mode participates in the soft-mode motion by an admix-

ture of the  $Q^{IIA_1}$  normal mode due to strong anharmonicity. Furthermore, the  $Q^{IA_1}$ -type displacements can modulate the intradimer and the intralayer exchange interactions. This implies that they can shift the quantum critical point  $x = J'/J$  while increasing  $J'$  and decreasing  $J$  and vice versa. Because of the orthogonal and frustrated exchange topology and the predominant motions of the soft mode along the  $z$  direction, however, the spin gap and the quantum critical point will undergo only a small change. Rather, the interlayer interactions will be strongly modulated. However, the absolute strength of the interlayer interactions is small. All of these explain why the observed softening of optic-phonon modes is weak in spite of the possible contributions of the intradimer and the intralayer interactions to spin-phonon couplings.

Finally, we will discuss another aspect of the structural phase transition related to the magnetic behavior and the relevance of antisymmetric interaction. Pronounced buckling distortions for temperatures below  $T < T_c$  can lead to a modification of anisotropic magnetic properties via spin-lattice interactions. The experimental observation of forbidden ESR transitions,<sup>21</sup> a splitting of the first triplet excitation into three branches,<sup>19</sup> and the unusual field dependence of magnetization plateaus<sup>33</sup> are not in accordance with a Shastry-Sutherland model based on isotropic superexchange. To explain the anomalous behaviors C epas *et al.*<sup>20</sup> derived the DM interactions from a simplified 2D spin model (corresponding to the HT phase), which lift partially the magnetic frustration as well as the degeneracy of the localized triplets.

However, we highlight that the presence of the bucking distortions in the LT phase leads to a complicated form of the DM interactions. In contrast to the assumption of C epas *et al.*,<sup>20</sup> the LT phase loses  $m_z$ ,  $m_y$ , and  $m_x$  mirror planes (see Sec. III A). Thus, for the purpose of a more complete description of anisotropic interactions we have performed a symmetry analysis using the exact symmetry of the LT phase. The exchange tensor of the intradimer interaction between copper ions 1 and 3 yields

$$J_{13}^{ij} = \begin{pmatrix} J_{13}^{xx} & d_{13}^z & D_{13}^y \\ d_{13}^z & J_{13}^{yy} & D_{13}^x \\ -D_{13}^y & -D_{13}^x & J_{13}^{zz} \end{pmatrix}, \quad (6)$$

where  $d_{ij}$  and  $D_{ij}$  denote the component of symmetric and antisymmetric anisotropic (Dzyaloshinskii-Moriya) interactions, respectively. Here note that in the HT phase only the symmetric anisotropic interaction of  $d_{13}^z$  is present. An upper conventional estimation<sup>34</sup> is given by  $d_{13}^z = (\Delta g/g)^2 J_{13} = 1.3$  K with the deviation of the  $g$  factor from  $2\Delta g = 0.28$  (Ref. 21) and  $J_{13} = J = 85$  K.<sup>2</sup> The appearance of the  $x$  and  $y$  components of DM interactions should be ascribed to a corrugation of the  $ab$  plane which includes Cu(1)-O<sub>*i*</sub>(2)-Cu(3) and Cu(1)-O<sub>*i*</sub>(4)-Cu(3) exchange interaction paths. At 100 K the angle between the  $ab$  plane and the plane including exchange paths amounts to  $\varphi = 3.5^\circ$ .<sup>15</sup> This allows an estimation of the strength of the DM interactions:<sup>34</sup>  $D_{13}^{y,x} = \sin \varphi (\Delta g/g) J_{13} = 0.63$  K. Because of the symmetricity of  $D_{13}^y = D_{13}^x$  the orientation of the DM vector lies along the

intradimer bond. The magnitude of the DM vector has a strong dependence on in-phase motions of  $O_i(2)$  and  $O_i(4)$  ions along the  $z$  direction. In addition, under a continuous corrugation of the  $\text{Cu-BO}_3$  layer the interdimer interactions will also undergo an appreciable modulation. From the symmetry analysis one obtains the exchange tensor of interdimer interactions between copper ions 1 and 2:

$$J_{12}^{ij} = \begin{pmatrix} J_{12}^{xx} & D_{12}^z & D_{12}^y \\ -D_{12}^z & J_{12}^{yy} & d_{12}^x \\ -D_{12}^y & d_{12}^x & J_{12}^{zz} \end{pmatrix}. \quad (7)$$

It is worth noting that only the antisymmetric component  $D_{12}^z$  is present in the HT phase. In contrast, in the LT phase  $D_{12}^y$  and  $d_{12}^x$  components appear. An estimation of their magnitude was not done due to the presence of complicated exchange paths of the interdimer interactions. The analysis of the interlayer exchange tensors has not been pursued because of their weak strength.

Our symmetry analysis shows the presence of the symmetric anisotropic  $z$  component of the intradimer interaction as well as the antisymmetric anisotropic  $z$  component of the interdimer interaction in the HT phase. The latter is suggested by the analysis of the 2D spin model by C epas *et al.*<sup>20</sup> To our best knowledge, until now the former has not been considered in the theoretical work. It can remove partially the frustration because its orientation is directed antiparallel to the nearest-neighboring dimers. In the LT phase the buckling distortions induce additionally the antisymmetric anisotropic  $x$  and  $y$  components of the intradimer interaction as well as the symmetric anisotropic  $x$  component of the interdimer interaction. The estimated value of  $D_{x,y} \sim 0.6$  K at 100 K is not negligible compared to  $D_z \approx 2$  K.<sup>20</sup> Therefore, we can conclude that a modulation of anisotropic interactions via spin-lattice couplings leads to an enhanced hopping of localized triplets and a mixing of triplet and singlet states. Thus,  $\text{SrCu}_2(\text{BO}_3)_2$  lies closer to the quantum critical point (to long-range order) than predicted based on pure 2D spin models.

#### IV. CONCLUSIONS

We have presented a Raman-scattering study of  $\text{Sr}_{1-x}\text{Ba}_x\text{Cu}_2(\text{BO}_3)_2$  ( $x=0$  and  $0.1$ ) in interlayer polarizations. With decreasing temperatures through the structural transition, a pronounced interlayer soft mode is observed. A symmetry analysis shows that this soft mode has an  $A_1$  symmetry corresponding to in-phase motions of almost all ions along the interlayer direction. This explains the extreme anisotropy of the Raman tensor of the soft mode as well as its low energy. The doping dependence further confirms this. In addition, a displacement of atomic motions along the  $z$  direction leads to a small modulation of the intralayer and the interlayer interactions as well as the appearance of additional symmetric and antisymmetric anisotropic interactions. For temperatures below the spin gap such a modulation results in an additional softening of the soft mode by 3%, indicating strong spin-phonon coupling. In particular, the buckling dis-

tortions and the special topology of  $\text{SrCu}_2(\text{BO}_3)_2$  lead to the coupling of spin to the soft optical phonon by exchange modulation. Our results show that in a realistic model for  $\text{SrCu}_2(\text{BO}_3)_2$  spin-phonon interactions, DM interactions, and interlayer lattice dynamics should be taken into account to understand a variety of physical properties such as the spin gap, the proximity to a quantum critical point, and anomalous behavior of the spectroscopic data. As a result,  $\text{SrCu}_2(\text{BO}_3)_2$  is closer to a quantum critical point than previously predicted.

#### ACKNOWLEDGMENTS

We thank C. Baumann for helpful discussions. This work was supported by DFG/SPP 1073 and NATO Collaborative Linkage Grant No. PST.CLG.977766.

#### APPENDIX

Here we list some normal coordinates which are relevant for the analysis of the structural and magnetic properties of  $\text{SrCu}_2(\text{BO}_3)_2$ .

Low-temperature phase,  
4*i*—positions (Cu, B, and O1 ions),  
 $A_1$ —irreducible representation,

$$Q_i^{IA_1} = \frac{1}{2\sqrt{2}}(-U_{1xy} + U_{2\bar{xy}} + U_{3xy} - U_{4\bar{xy}}),$$

$$Q_i^{IIA_1} = \frac{1}{2}(U_{1z} - U_{2z} + U_{3z} - U_{4z}),$$

$A_2$ —irreducible representation,

$$Q_i^{A_2} = \frac{1}{2\sqrt{2}}(-U_{1\bar{xy}} - U_{2xy} + U_{3\bar{xy}} + U_{4xy}),$$

$B_1$ —irreducible representation,

$$Q_i^{B_1} = \frac{1}{2\sqrt{2}}(-U_{1\bar{xy}} + U_{2xy} + U_{3\bar{xy}} - U_{4xy}),$$

$B_2$ —irreducible representation,

$$Q_i^{IB_2} = \frac{1}{2\sqrt{2}}(-U_{1xy} - U_{2\bar{xy}} + U_{3xy} + U_{4\bar{xy}}),$$

$$Q_i^{IIB_2} = \frac{1}{2}(U_{1z} + U_{2z} + U_{3z} + U_{4z}),$$

$E$ —irreducible representation;

$$Q_{1,i}^{IE} = \frac{1}{2}(U_{1x} + U_{2x} + U_{3x} + U_{4x}),$$

$$Q_{2,i}^{IE} = -\frac{1}{2}(U_{1y} + U_{2y} + U_{3y} + U_{4y}),$$

$$Q_{1,i}^{\text{II}E} = \frac{1}{2}(U_{1y} - U_{2y} + U_{3y} - U_{4y}),$$

$$Q_{2,i}^{\text{II}E} = \frac{1}{2}(-U_{1x} + U_{2x} - U_{3x} + U_{4x}),$$

$$Q_{1,i}^{\text{III}E} = \frac{1}{2}(U_{1z} - U_{2z} - U_{3z} + U_{4z}),$$

$$Q_{2,i}^{\text{III}E} = \frac{1}{2}(-U_{1z} - U_{2z} + U_{3z} + U_{4z}),$$

$A_1$ —irreducible representation for  $8j$  positions,

$$Q_j^{\text{IA}_1} = \frac{1}{4}(U_{1xy} + U_{2xy} - U_{3\bar{xy}} - U_{4\bar{xy}} \\ - U_{5xy} + U_{6xy} + U_{7\bar{xy}} + U_{8\bar{xy}}),$$

$$Q_j^{\text{II}A_1} = \frac{1}{4}(-U_{1\bar{xy}} + U_{2\bar{xy}} - U_{3xy} + U_{4xy} \\ + U_{5\bar{xy}} - U_{6\bar{xy}} + U_{7xy} - U_{8xy}),$$

$$Q_j^{\text{III}A_1} = \frac{1}{2\sqrt{2}}(U_{1z} + U_{2z} - U_{3z} \\ - U_{4z} + U_{5z} + U_{6z} - U_{7z} - U_{8z}),$$

High-temperature phase,

$B_{1u}$ —irreducible representation for  $4h$  positions,

$$Q_h^{B_{1u}} = \frac{1}{2}(U_{1z} - U_{2z} + U_{3z} - U_{4z}) = Q_i^{\text{II}A_1}$$

$E_g$ —irreducible representation for  $4h$  positions,

$$Q_{1,h}^{E_g} = \frac{1}{2}(U_{1z} - U_{2z} - U_{3z} + U_{4z}) = Q_{1,i}^{\text{III}E},$$

$$Q_{2,h}^{E_g} = \frac{1}{2}(-U_{1z} - U_{2z} + U_{3z} + U_{4z}) = Q_{2,i}^{\text{III}E},$$

$E_u$ —irreducible representation for  $4h$  positions,

$$Q_{1,h}^{IE_u} = \frac{1}{2}(U_{1x} + U_{2x} + U_{3x} + U_{4x}) = Q_{1,i}^{IE},$$

$$Q_{2,h}^{IE_u} = -\frac{1}{2}(U_{1y} + U_{2y} + U_{3y} + U_{4y}) = Q_{2,i}^{IE},$$

$$Q_{1,h}^{\text{II}E_u} = \frac{1}{2}(U_{1y} - U_{2y} + U_{3y} - U_{4y}) = Q_{1,i}^{\text{II}E},$$

$$Q_{2,h}^{\text{II}E_u} = \frac{1}{2}(-U_{1x} + U_{2x} - U_{3x} + U_{4x}) = Q_{2,i}^{\text{II}E},$$

$B_{1u}$ —irreducible representation for  $8k$  positions,

$$Q_k^{B_{1u}} = \frac{1}{2\sqrt{2}}(U_{1z} + U_{2z} - U_{3z} \\ - U_{4z} + U_{5z} + U_{6z} - U_{7z} - U_{8z}).$$

- 
- <sup>1</sup>B.S. Shastry and B. Sutherland, *Physica B & C* **108**, 1069 (1981).  
<sup>2</sup>S. Miyahara and K. Ueda, *J. Phys.: Condens. Matter* **15**, R327 (2003).  
<sup>3</sup>A. Koga and N. Kawakami, *Phys. Rev. Lett.* **84**, 4461 (2000).  
<sup>4</sup>S. Miyahara and K. Ueda, *Phys. Rev. Lett.* **82**, 3701 (1999).  
<sup>5</sup>H. Kageyama, K. Yoshimura, R. Stern, N.V. Mushnikov, K. Onizuka, M. Kato, K. Kosuge, C.P. Slichter, T. Goto, and Y. Ueda, *Phys. Rev. Lett.* **82**, 3168 (1999).  
<sup>6</sup>H. Kageyama, M. Nishi, N. Aso, K. Onizuka, T. Yoshida, K. Nukui, K. Kodama, K. Kakurai, and Y. Ueda, *Phys. Rev. Lett.* **84**, 5876 (2000).  
<sup>7</sup>P. Lemmens, M. Grove, M. Fischer, G. Güntherodt, V.N. Kotov, H. Kageyama, K. Onizuka, and Y. Ueda, *Phys. Rev. Lett.* **85**, 2605 (2000).  
<sup>8</sup>E. Müller-Hartmann, R.R.P. Singh, C. Knetter, and G.S. Uhrig, *Phys. Rev. Lett.* **84**, 1808 (2000).  
<sup>9</sup>W. Zheng, J. Oitmaa, and C.J. Hamer, *Phys. Rev. B* **65**, 014408 (2001), and references therein.  
<sup>10</sup>H. Kageyama, *Physica B* **329-333**, 1020 (2003).  
<sup>11</sup>P. Lemmens, G. Güntherodt, and C. Gros, *Phys. Rep.* **375**, 1 (2003).  
<sup>12</sup>Ch. Knetter, A. Bühler, E. Müller-Hartmann, and G.S. Uhrig, *Phys. Rev. Lett.* **85**, 3958 (2000).  
<sup>13</sup>Sh. Miyahara and K. Ueda, *J. Phys. Soc. Jpn.* **69**, 72 (2000).  
<sup>14</sup>A. Koga, *J. Phys. Soc. Jpn.* **69**, 3509 (2000).  
<sup>15</sup>K. Sparta, G.J. Redhammer, P. Roussel, G. Heger, G. Roth, P. Lemmens, A. Ionescu, M. Grove, G. Güntherodt, F. Hüning, H. Lueken, H. Kageyama, K. Onizuka, and Y. Ueda, *Eur. Phys. J. B* **19**, 507 (2001).  
<sup>16</sup>S. Miyahara and K. Ueda, *Phys. Rev. Lett.* **82**, 3701 (1999).  
<sup>17</sup>B. Wolf, S. Zherlitsyn, S. Schmidt, B. Lüthi, H. Kageyama, and Y. Ueda, *Phys. Rev. Lett.* **86**, 4847 (2001).  
<sup>18</sup>K. Kodama, M. Takigawa, M. Horvatic, C. Berthier, H. Kageyama, Y. Ueda, S. Miyahara, F. Becca, and F. Mila, *Science* **298**, 395 (2002).  
<sup>19</sup>N. Aso, H. Kageyama, K. Nukui, M. Nishi, K. Kakurai, K. Onizuka, Y. Ueda, and H. Kadowaki, *J. Phys. Chem. Solid.* (to be published).  
<sup>20</sup>O. Cépas, K. Kakurai, L.P. Regnault, T. Ziman, J.P. Boucher, N. Aso, M. Nishi, H. Kageyama, and Y. Ueda, *Phys. Rev. Lett.* **87**, 167205 (2001).  
<sup>21</sup>H. Nojiri, H. Kageyama, K. Onizuka, Y. Ueda, and M. Motokawa, *J. Phys. Soc. Jpn.* **68**, 2906 (1999).  
<sup>22</sup>K. Totsuka, S. Miyahara, and K. Ueda, *Phys. Rev. Lett.* **86**, 520 (2001).  
<sup>23</sup>H. Kageyama, K. Onizuka, T. Yamauchi, and Y. Ueda, *J. Cryst. Growth* **206**, 65 (1999).

- <sup>24</sup>M. Grove, P. Lemmens, G. Güntherodt, B.C. Sales, F. Bülesfeld, and W. Assmus, *Phys. Rev. B* **61**, 6126 (2000).
- <sup>25</sup>J. Kikuchi, K. Motoya, T. Yamauchi, and Y. Ueda, *Phys. Rev. B* **60**, 6731 (1999).
- <sup>26</sup>T. Saito *et al.*, *J. Solid State Chem.* **153**, 124 (2000).
- <sup>27</sup>G.S. Uhrig and B. Normand, *Phys. Rev. B* **63**, 134418 (2001).
- <sup>28</sup>M. Balkanski, R.F. Wallis, and E. Haro, *Phys. Rev. B* **28**, 1928 (1983).
- <sup>29</sup>V.L. Ginzburg, A.P. Levanyuk, and A.A. Sobyenin, *Phys. Rep.* **57**, 151 (1980).
- <sup>30</sup>M. Braden, B. Hennion, W. Reichardt, G. Dhalenne, and A. Revcolevschi, *Phys. Rev. Lett.* **80**, 3634 (1998).
- <sup>31</sup>S. Zherlitsyn, S. Schmidt, B. Wolf, H. Schwenk, B. Lüthi, H. Kageyama, K. Onizuka, Y. Ueda, and K. Ueda, *Phys. Rev. B* **62**, R6097 (2000).
- <sup>32</sup>Sh. Miyahara, F. Becca, and F. Mila, cond-mat/0302332 (unpublished).
- <sup>33</sup>K. Onizuka, H. Kageyama, Y. Narumi, K. Kindo, Y. Ueda, and T. Goto, *J. Phys. Soc. Jpn.* **69**, 1016 (2000).
- <sup>34</sup>T. Moriya, *Phys. Rev.* **120**, 91 (1960).